The following appendices accompany the article

Planktonic food webs: microbial hub approach

Louis Legendre[1,2,*], Richard B. Rivkin[3]

[1]UPMC Univ Paris 06, UMR 7093, Laboratoire d'Océanographie de Villefranche, 06230 Villefranche-sur-Mer, France
[2]CNRS, UMR 7093, LOV, 06230 Villefranche-sur-Mer, France
[3]Ocean Sciences Centre, Memorial University of Newfoundland, St. John's, Newfoundland A1C 5S7, Canada

*Email: legendre@obs-vlfr.fr

Marine Ecology Progress Series 365:289–309 (2008)

Appendix 1. Development of the food-web model and of the microbial-hub approach

Definition of model parameters

Although our steady-state model was not designed to reproduce field observations, we used representative values for the parameters (i.e. between-compartment flows). The notations used are in Table 1; the additional notations used only in this appendix are in Table A1 (figures, tables, and equations with the 'A' designation are in this appendix; those without are in the text). The parameters for the 7 steps of the model illustrated in Figs. 1a & 3 were determined as described below; values are given in Table A2. In our model, parameter flows out of a compartment are expressed as a function of the total input flow (A or I) into that compartment, whereas modeled flows are expressed as a function of PP_T or R_C ($PP_T = R_C$).

We partitioned total primary production between the particulate and dissolved fractions as PP_P:PP_D = 0.8:0.2, to reflect the published global median values as described in Appendix 2. We computed Step 7 of the model for the 5 planktonic food webs described in the text. The difference in parameterization among 5 modeled food webs is in their respective flows from PHYTO/POC to MZOO (PP_{Pmz}) and to µZOO ($PP_{P\mu z}$) (Table A2).

The 3 heterotrophic compartments (i.e. BACT, µZOO, and MZOO) were made temperature (T)-dependent, by scaling their growth efficiencies to T.

Table A1. Notations for variables, flows of organic carbon (parameters and modeled), and subscripts used in this appendix, in addition to those given in Table 1

Notation	Variable, flow, model parameter
T	Temperature
BLMF	Bacterial lysis mortality factor
Subscript	**Meaning**
PL	Large-sized *PP*:total *PP*

The values of the parameters used in our models without viral lysis, at 15°C, are given in Table A2.

For the BACT compartment, we used the BGE = $f(T)$ relationship of Rivkin & Legendre (2001):

$$\mathrm{BGE} = 0.374 - 0.0104 \times T \quad \text{(A1)}$$

Because we did not consider viral lysis of bacteria at this stage of the modeling (i.e. $L_b = 0$), BGE_1 (Eq. 9) = BGE_2 (Eq. 10) = BGE (Eq. A1). With Eq. (A1), we computed the 2 T-dependent parameter flows from BACT, i.e. P_b/A_b and R_b/A_b:

$$P_b/A_b = \mathrm{BGE} \quad \text{(A2)}$$

$$R_b/A_b = 1 - (P_b/A_b) = 1 - \mathrm{BGE} \quad \text{(A3)}$$

Eq. (A2) is based on Eq. (A1) and Eqs. (9 & 10), and Eq. (A3) is based on Eq. (A2) and Eq. (A32, in Electronic Appendix 2).

For the µZOO compartment, we used the $GGE_{\mu z} = f(T)$ relationship of Rivkin & Legendre (2001):

$$\mathrm{GGE}_{\mu z} = 0.66 - 0.014 \times T \quad \text{(A4)}$$

The 3 T-dependent parameter flows from µZOO are: $P_{\mu z}/I_{\mu z}$, $E_{\mu z}/I_{\mu z}$, and $R_{\mu z}/I_{\mu z}$. With Eq. (A4), we computed the $P_{\mu z}/I_{\mu z}$ parameter:

$$P_{\mu z}/I_{\mu z} = \mathrm{GGE}_{\mu z} \quad \text{(A5)}$$

Eq. (A5) is based on Eqs. (A4) & (6). The sum of the 2 remaining µZOO parameters is $(E_{\mu z}/I_{\mu z} + R_{\mu z}/I_{\mu z}) = [1 - (P_b/I_b)]$. To compute the individual values of the 2 parameters, we treated $E_{\mu z}/I_{\mu z}$ and $R_{\mu z}/I_{\mu z}$ as 2 parallel flows out of the µZOO compartment, i.e. we partitioned $[1 - (P_b/I_b)]$ between $E_{\mu z}/(E_{\mu z} + R_{\mu z})$ and $R_{\mu z}/(E_{\mu z} + R_{\mu z})$. To obtain $E_{\mu z}/(E_{\mu z} + R_{\mu z})$, we used $R_{\mu z}/I_{\mu z}$ and $E_{\mu z}/I_{\mu z}$ values of 0.33 and 0.44, respectively (Pelegrí et al. 1999; heterotrophic nanoflagellate *Pteridomonas danica* feeding on *Escherichia coli*). From these values, we calculated:

$$E_{\mu z}/(E_{\mu z} + R_{\mu z}) = 0.6 \quad \text{(A6)}$$

We checked the general applicability of this 0.6 value by comparing the corresponding $E_{\mu z}/I_{\mu z}$ with those reported by Strom et al. (1997; their Fig. 4) for a ciliate

Table A2. Parameters (flows out of compartments) for the 7 steps of the steady-state food-web model illustrated in Figs. 1a & 3, and described in Table 4 (without viral lysis, 15°C). Values in the present table specify each output flow from a compartment, and are expressed as a fraction of the total input flows into that compartment. The sum of parameter flows out of any compartment is 1. ∅ indicates that the flow does not exist in the given model. The 5 last columns are versions of Model Step 7, corresponding to the extreme microbial (ExMi), microbial (Micr), multivorous (Mult), herbivorous (Herb), and extreme herbivorous (ExHe) food webs. Because in our model PP_D, $E_{\mu z}$, and E_{mz} are channeled directly to BACT, the DOC compartment is not modeled explicitly

Parameter	1	2	3	4	5	6	ExMi	Micr	Mult	Herb	ExHe
P_b/A_b	∅	∅	∅	0.218	0.218	0.218	0.218	0.218	0.218	0.218	0.218
R_b/A_b	1.000	1.000	1.000	0.782	0.782	0.782	0.782	0.782	0.782	0.782	0.782
D_b/D	∅	∅	∅	∅	∅	∅	0.600	0.600	0.600	0.600	0.600
D_{mz}/D	∅	∅	∅	∅	∅	∅	0.400	0.400	0.400	0.400	0.400
R_{large}/I_{large}	∅	∅	1.000	1.000	1.000	1.000	1.000	1.000	1.000	1.000	1.000
$E_{\mu z}/I_{\mu z}$	∅	∅	∅	∅	0.330	0.330	0.330	0.330	0.330	0.330	0.330
$P_{\mu z}/I_{\mu z}$	∅	0.450	0.450	0.450	0.450	0.450	0.450	0.450	0.450	0.450	0.450
$R_{\mu z}/I_{\mu z}$	∅	0.550	0.550	0.550	0.220	0.220	0.220	0.220	0.220	0.220	0.220
F_{mz}/I_{mz}	∅	∅	∅	∅	∅	∅	0.300	0.300	0.300	0.300	0.300
E_{mz}/I_{mz}	∅	∅	∅	∅	∅	0.148	0.148	0.148	0.148	0.148	0.148
P_{mz}/I_{mz}	∅	∅	0.249	0.249	0.249	0.249	0.249	0.249	0.249	0.249	0.249
R_{mz}/I_{mz}	1.000	1.000	0.752	0.752	0.752	0.603	0.303	0.303	0.303	0.303	0.303
PP_D/PP_T	0.200	0.200	0.200	0.200	0.200	0.200	0.200	0.200	0.200	0.200	0.200
$PP_{P\mu z}/PP_p$	0.000	0.650	0.650	0.650	0.650	0.650	1.000	0.900	0.650	0.250	0.000
PP_{Pmz}/PP_p	1.000	0.350	0.350	0.350	0.350	0.350	0.000	0.100	0.350	0.750	1.000

feeding on a flagellate at 12°C (i.e. $E_{\mu z}/I_{\mu z} \geq 0.3$; experimental results corrected for bacterial consumption of DOC with BGE = 0.25), and by Nagata (2000) based on a survey of the literature (i.e. $0.1 < E_{\mu z}/I_{\mu z} < 0.3$). We computed $E_{\mu z}/I_{\mu z}$ at 12°C corresponding to Eq. (A6) by combining Eqs. (A4 & A5), which gave $(R_{\mu z} + E_{\mu z})/I_{\mu z} = 0.5$, and multiplied the latter value by $E_{\mu z}/(E_{\mu z} + R_{\mu z}) = 0.6$ (Eq. A6), which gave $E_{\mu z}/I_{\mu z} = 0.3$. This value is at the low and high ends of the ranges of $E_{\mu z}/I_{\mu z}$ reported by Strom et al. (1997) and Nagata (2000), respectively, suggesting that the 0.6 value from Pelegrí et al. (1999) is generally applicable. We computed the $E_{\mu z}/I_{\mu z}$ parameter as follows:

$$E_{\mu z}/I_{\mu z} = [E_{\mu z}/(E_{\mu z} + R_{\mu z})] \times (1 - P_{\mu z}/I_{\mu z}) \quad (A7)$$

Eq. (A7) is derived from Eq. (3). Using Eq. (A6), Eq. (A7) becomes:

$$E_{\mu z}/I_{\mu z} = 0.6 \times (1 - P_{\mu z}/I_{\mu z}) = 0.6 \times (1 - GGE_{\mu z}) \quad (A8)$$

We computed the $R_{\mu z}/I_{\mu z}$ parameter as:

$$R_{\mu z}/I_{\mu z} = 1 - (P_{\mu z}/I_{\mu z} + E_{\mu z}/I_{\mu z}) = 0.4 \times (1 - GGE_{\mu z}) \quad (A9)$$

Eq. (A9) combines Eqs. (A5 & A8) and Eq. (3).

For the MZOO compartment, we computed the parameter flow to DETR using $AE_{mz} = 0.7$ of Ikeda & Motoda (1978):

$$F_{mz}/I_{mz} = 1 - AE_{mz} = 0.3 \quad (A10)$$

Eq. (A10) combines Eqs. (1) & (7). The 3 other MZOO parameters were made T-dependent by using the $NGE_{mz} = f(T)$ relationship of Legendre & Rivkin (2005, values for LZ in their Table 4):

$$NGE_{mz} = 0.40 - 0.003 \times T \quad (A11)$$

This empirical relationship was derived from the DW = $f(T)$ and NGE = f(DW, T) values in Table 2 and Fig. 3, respectively, of Ikeda et al. (2001), where DW is the dry weights of copepods. The 3 T-dependent parameter flows from MZOO are: P_{mz}/I_{mz}, E_{mz}/I_{mz}, and R_{mz}/I_{mz}. We computed the P_{mz}/I_{mz} parameter as follows:

$$P_{mz}/I_{mz} = GGE_{mz} = NGE_{mz} \times AE_{mz} \quad (A12)$$

Eq. (A12) is based on Eq. (A11) and Eqs. (5 to 8). We set the parameter $E_{mz}/I_{mz} = 0.15$ at 15°C. This value is at the lower end of the range of E_{mz}/I_{mz} reported by Strom et al. (1997; their Fig. 4) for a copepod feeding on phytoplankton at 12°C (i.e. $E_{mz}/I_{mz} \geq 0.15$; experimental results corrected for BGE = 0.25), and within the range reported by Nagata (2000; i.e. $0.1 < E_{mz}/I_{mz} < 0.2$). In order to treat E_{mz}/I_{mz} in the same way as the $E_{\mu z}/I_{\mu z}$ parameter (Eq. A7), we first expressed E_{mz} as a fraction of $(E_{mz} + R_{mz})$. Using Eqs. (2), (5) & (7), it can be shown that:

$$E_{mz}/(E_{mz} + R_{mz}) = (E_{mz}/A_{mz})/(1 - NGE_{mz}) = [(E_{mz}/I_{mz})/AE_{mz}]/(1 - NGE_{mz}) \quad (A13)$$

Because $E_{mz}/I_{mz} = 0.15$, $AE_{mz} = 0.7$ and $NGE_{mz} = 0.36$ at 15°C (Eq. A11), Eq. (A13) resolves to:

$$E_{mz}/(E_{mz} + R_{mz}) = 0.33 \quad (A14)$$

The equation for the E_{mz}/I_{mz} parameter is parallel to Eq. (A7) for µZOO:

$$E_{mz}/I_{mz} = AE_{mz} \times [E_{mz}/(E_{mz} + R_{mz})] \times (1 - P_{mz}/A_{mz}) = [E_{mz}/(E_{mz} + R_{mz})] \times (AE_{mz} - P_{mz}/I_{mz}) \quad (A15)$$

Eq. (A15) is based on Eq. (A14) and Eqs. (2 & 7). Given Eq. (A14), $AE_{mz} = 0.7$ and $P_{mz}/A_{mz} = NGE_{mz}$ (Eq. 5), Eq. (A15) becomes:

$$E_{mz}/I_{mz} = 0.23 \times (1 - NGE_{mz}) = 0.33 \times (0.7 - P_{mz}/I_{mz}) \quad (A16)$$

The equation for the R_{mz}/I_{mz} parameter is parallel to Eq. (A9) for µZOO:

$$R_{mz}/I_{mz} = 1 - (F_{mz}/I_{mz} + P_{mz}/I_{mz} + E_{mz}/I_{mz}) \quad (A17)$$

Eq. (A17) combines Eqs. (A10), (A12) & (A16) and Eq. (3).

All components of the planktonic food web consume varying amounts of organic detritus. In our model, there are 2 pathways leading from detritus to both bacterial use of DOC released from fecal pellets, and use of particulate detritus by mesozooplankton and bacteria. Given these known pathways, we partitioned the organic detritus (D) between bacteria and mesozooplankton (D_b/D and D_{mz}/D) in the proportion 0.6:0.4. The remaining parameter in Table A2, i.e. metazoan respiration (R_{metaz}), was set to 1.0 by model construction.

Fig. A1 compares the temperature dependence of BGE, $GGE_{\mu z}$, NGE_{mz}, and GGE_{mz} (assuming $AE_{mz} = 0.7$), as defined by Eqs. (A1), (A4), (A11) & (A12). The figure shows that, in our model, BACT and µZOO respond similarly to temperature (similar slopes), and these 2 compartments are more temperature dependent (higher slopes) than MZOO.

Computation of steady-state solution

The steady-state solution for each run of the model was computed as follows. Each modeled output flow was expressed as a linear function of the relevant flow parameters, and all flow equations were written in the same row of a Microsoft Excel spreadsheet. Because there are backward flows in the model (i.e. E and F; Figs. 1 & 5), the Excel solution required multiple iterations. This was achieved by activating the 'Iteration' feature of Excel (up to 1000 iterations). All output flows corresponding to the steady-state solution were thus modeled simultaneously.

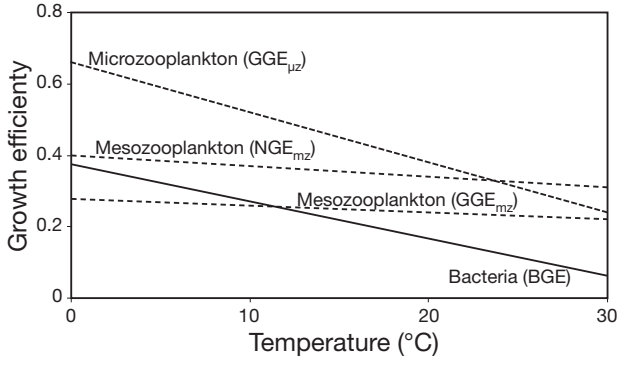

Fig. A1. Temperature dependence of the 4 growth efficiencies used in the model. GGE_{mz} was calculated from NGE_{mz} assuming $AE_{mz} = 0.7$ (Eq. A12)

Comparisons with other studies

Table A3 compares the values of parameters at Step 7 of our model (multivorous food web, without viral lysis; Table A2) and in the model of Anderson & Ducklow (2001). Although the parameters were determined quite differently in the 2 studies, the 2 sets of parameter values are remarkably similar.

Our modeled flows A and R of BACT + µZOO for the 5 planktonic food webs at 15°C (Table 6) are ($P_b + R_b + P_{\mu z} + R_{\mu z} + E_{\mu z}$) = 68 to 162% and ($R_b + R_{\mu z}$) = 56 to 67% of PP_T, respectively. These modeled values are similar to the field-based values summarized in Table 3 for BACT and µZOO in 3 zones of the world ocean (i.e. $\sum A/PP_T$ = 112 to 142% and $\sum R/PP_T$ = 67 to 96%). In addition, values of BACT carbon demand reported in Table 6 (i.e. $P_b + R_b$ = 0.56 to 0.67) are similar to those reported by Anderson & Ducklow (2001; i.e. BCD-*PP* at the bottom of their Fig. 4) for the steady-state subarctic North Pacific (0.68), Equatorial Pacific (1.70), and Sargasso Sea (0.79), especially that these authors included viral lysis of BACT in their model, and we did not.

Viral lysis of bacteria

In our steady-state model (Figs. 1a & 5), all P_b is consumed by µZOO, i.e. P_b is the grazer-mediated BACT mortality. Recent studies suggest that up to half of BACT mortality may be due to viral lysis. In order to assess the effect of L_b on food-web processes, we added to our model (Fig. 3, Table 4) a simple 'lysis loop' (Fig. 4), which implements the partitioning of A_b among P_b, R_b, and L_b as discussed in the text (Eq. 4, Fig. 2c).

Because in steady-state models, the biomasses of compartments are constant, grazing-mediated BACT mortality in our model is equal to P_b. Consequently, when there is mortality due to viral lysis, total BACT mortality is equal to ($P_b + L_b$). Here, we define a bacterial lysis mortality factor (BLMF):

$$BLMF = L_b/(P_b + L_b) \quad (A18)$$

This factor will be used to calculate the BACT parameters required to run the model with viral lysis, i.e. P_b/A_b, R_b/A_b, and L_b/A_b. It follows from Eq. (4) that:

Table A3. Values of parameters for our steady-state Model Step 7 for the multivorous food web, without lysis at 15°C (Table A2, Figs. 1a & 3), and that of Anderson & Ducklow (2001). The model of Anderson & Ducklow (2001) considers only 1 size class each for phytoplankton and zooplankton; symbols are defined in their paper. ∅ indicates that the flow does not exist in the given model

Parameter	Present study Value	Anderson and & Ducklow (~~2001~~) Value	Definition
PER	0.2	0.17, 0.56, 0.27	{PER [0.13, 0.54, 0.23] × (1 – ξ_P)} + ξ_P [0.05]
L_b/A_b	∅	0.07, 0.02, 0.04	ξ_B [0.25] × ω [0.27, 0.09, 0.14]
P_b/A_b	0.22	0.20, 0.07, 0.11	(1 – ξ_B) × ω
R_b/A_b	0.78	0.73, 0.91, 0.86	(1 – ω)
D_b/D	0.6	1	
D_{mz}/D	0.4	0	
R_{large}/I_{large}	1	1	
$E_{\mu z}/I_{\mu z}$	0.33	∅	
$P_{\mu z}/I_{\mu z}$	0.45	∅	
$R_{\mu z}/I_{\mu z}$	0.22	∅	
F_{mz}/I_{mz}	0.3	0.25	1 – AE [0.75]
E_{mz}/I_{mz}	0.15	0.05	ϕ_1 [0.3] – (1 – AE)
P_{mz}/I_{mz}	0.25	0.25	k_c [0.36] × (1 – ϕ_1)
R_{mz}/I_{mz}	0.3	0.45	(1 – ϕ_1) – $P_{\mu z}$
$PP_{P\mu z}/PP_p$	0.65	∅	
PP_{Pmz}/PP_p	0.35	1	

was the same in the absence and the presence of lysis, i.e. these models used $BGE_2 = (P_b + L_b)/(P_b + R_b + L_b)$ (Eq. 10). It can be shown from Eqs. (4), (10) & (A18) that the corresponding equations for L_b/A_b and P_b/A_b are:

$$L_b/A_b = BGE_2 \times BLMF \quad (A20)$$

$$P_b/A_b = BGE_2 \times (1 - BLMF) \quad (A21)$$

BACT parameters R_b/A_b, L_b/A_b, and P_b/A_b are defined by Eqs. (A19) to (A21); Table A4 gives the values of modeled flows in the absence (BLMF = 0.0) and in the presence (BLMF = 0.4) of viral lysis of BACT, calculated with Eqs. (A19) to (A21), for the 5 food webs. BGE_2 was assumed to have the same value as BGE calculated with Eq. (A1) at 15°C. Results are discussed in the text.

As further explained in the text, we also ran our model with the alternative assumption of constant $BGE_1 = P_b/(P_b + R_b)$ (Eq. 9). In this case, it can be shown from Eq. (A18) and Eq. (9) that the equations for L_b/A_b, and P_b/A_b are:

$$R_b/A_b = 1 - (P_b/A_b) - (L_b/A_b) \quad (A19)$$

$$L_b/A_b = BGE_1 \times BLMF/[(1 - BLMF) + (BGE_1 \times BLMF)] \quad (A22)$$

$$P_b/A_b = BGE_1 \times [1 - (L_b/A_b)] \quad (A23)$$

Hence, to compute parameter R_b/A_b, one needs parameters P_b/A_b and L_b/A_b.

As explained in the text (section 'Model effects of DOC release from bacteria'), Fuhrman (1992, 1999) used steady-state models to explore the effects of viral lysis on carbon flows implicitly assuming that R_b/A_b

In summary, when BGE_1 is used, BACT parameters P_b/A_b, L_b/A_b, and R_b/A_b are calculated with Eqs. (A22), (A23) & (A19) respectively. Table A5 gives the values of modeled flows in the presence of viral

Table A4. Values of modeled flows under the assumption that R_b/A_b was the same in the absence (BLMF = 0.0) and in the presence (BLMF = 0.4) of viral lysis of BACT, i.e. constant BGE_2. Values were calculated with Eqs. (A19) to (A21), for the 5 food webs. BGE_2 was assumed to have the same value as BGE calculated with Eq. (A1) at 15°C. Bold values: difference ≥15% between BLMF = 0.0 and BLMF = 0.4

Food web	I_C	A_C	P_C	P_b	R_b	L_b	$P_{\mu z}$	$R_{\mu z}$	$E_{\mu z}$	P_{DOC}
Absence of viral lysis of bacteria (BLMF = 0.0)										
Extr. microb.	2.22	2.08	0.69	**0.15**	0.52	**0.00**	0.43	0.21	0.31	0.47
Microbial	2.19	2.03	0.66	**0.14**	0.52	**0.00**	0.39	0.19	0.29	0.46
Multivorous	2.11	1.91	0.60	**0.14**	0.49	**0.00**	0.30	0.14	0.22	0.43
Herbivorous	1.98	1.72	**0.49**	**0.13**	0.46	**0.00**	0.15	0.07	0.11	0.39
Extr. herb.	1.89	1.60	**0.42**	**0.12**	0.44	**0.00**	**0.05**	**0.03**	**0.04**	0.36
Presence of viral lysis of bacteria (BLMF = 0.4)										
Extr. microb.	2.17	2.03	0.61	**0.09**	0.55	**0.06**	0.40	0.20	0.29	0.44
Microbial	2.14	1.98	0.58	**0.09**	0.54	**0.06**	0.36	0.18	0.27	0.43
Multivorous	2.06	1.87	0.52	**0.09**	0.52	**0.06**	0.27	0.13	0.20	0.41
Herbivorous	1.93	1.68	**0.41**	**0.08**	0.48	**0.05**	0.13	0.06	0.09	0.36
Extr. herb.	1.85	1.56	**0.35**	**0.08**	0.46	**0.05**	**0.03**	**0.02**	**0.03**	0.34

Table A5. Values of modeled flows under the assumption of constant BGE_1 with viral lysis (BLMF = 0.4), calculated with Eqs. (A19), (A22) & (A23), for the 5 food webs at 15°C (Eq. A1). Values below are compared with those in the last 5 rows of Table 6 (i.e. modeled flows, with constant BGE_1, without lysis). The only values different from those in the last 5 rows of Table 6 are I_C, A_C, and L_b (in Table 6, $L_b = 0$)

Food web	I_C	A_C	P_C	P_b	R_b	L_b	$P_{\mu z}$	$R_{\mu z}$	$E_{\mu z}$	P_{DOC}
Extr. microb.	2.32	2.17	0.69	0.15	0.52	0.10	0.43	0.21	0.31	0.47
Microbial	2.28	2.13	0.66	0.14	0.52	0.10	0.39	0.19	0.29	0.46
Multivorous	2.20	2.00	0.60	0.14	0.49	0.09	0.30	0.14	0.22	0.43
Herbivorous	2.06	1.81	0.49	0.13	0.46	0.09	0.15	0.07	0.11	0.39
Extr. herb.	1.98	1.68	0.42	0.12	0.44	0.08	0.05	0.03	0.04	0.36

lysis (BLMF = 0.4), calculated with Eqs. (A22), (A23) & (A19), for the 5 food webs at 15°C (Eq. A1). These values are to be compared with those in the last 5 rows of Table 6. Results are discussed in the text.

Viral lysis of phytoplankton

As presented in the text (section 'Model effects of DOC release from bacteria'), some published models include the effects of viral lysis of both BACT and PHYTO (e.g. Fuhrman 1999, Wilhelm & Suttle 1999). To assess the effects of including PHYTO viral lysis, we ran our model with viral lysis of both BACT (BLMF = 0.4) and PHYTO (simulated by increasing PHYTO PER from 0.20 to 0.25). Table A6 gives the values of modeled flows for different runs of our model, for the multivorous food web at 15°C. The results show that, independently from the assumption concerning constant BGE_1 or BGE_2 (above), the addition of PHYTO viral lysis increases R_b and decreases the µZOO flows.

Phytodetritus

As explained in the text (section 'Effects of phytodetritus'), we did not initially consider the formation of phytodetritus in the euphotic zone. To examine a possible effect of this process on our modeled results, we ran the model assuming that 20% of PP_P was transferred to phytodetritus and 80% was consumed by µZOO and MZOO. Resulting modeled flows for the 5 planktonic food webs are given in Table A7, where they are compared with those in the last 5 rows of Table 6. Results are discussed in the text.

Table A6. Values of modeled flows for the multivorous food web at 15°C. Top rows: assumption of constant BGE_2; model runs without viral lysis, with viral lysis of BACT (BLMF = 0.4), and with viral lysis of both BACT and PHYTO (PHYTO PER increased from 0.20 to 0.25), respectively. Lower 3 rows: same model runs as above, with the assumption of constant BGE_1

Model run	I_C	A_C	P_C	P_b	R_b	L_b	$P_{\mu z}$	$R_{\mu z}$	$E_{\mu z}$
BGE_2 constant	2.11	1.91	0.60	0.14	0.49	0.00	0.30	0.14	0.22
+ BACT lysis	2.06	1.87	0.52	0.09	0.52	0.06	0.27	0.13	0.20
+ PHYTO lysis	2,02	1,84	0,50	0,09	0,54	0,06	0,26	0,13	0,19
BGE_1 constant	2.20	2.00	0.60	0.14	0.49	0.00	0.30	0.14	0.22
+ BACT lysis	2.20	2.00	0.60	0.14	0.49	0.09	0.30	0.14	0.22
+ PHYTO lysis	2.17	1.98	0.58	0.14	0.52	0.10	0.28	0.14	0.21

Table A7. Effects of phytodetritus on modeled flows (without viral lysis of bacteria). Values were computed with 20% of PP_P transferred to phytodetritus in the euphotic zone, and 80% of PP_P consumed by µZOO and MZOO. Values below are compared with those in the last 5 rows of Table 6 (i.e. modeled flows, without production of phytodetritus), and differences ≥15% are in bold

Food web	I_C	A_C	P_C	P_b	R_b	$P_{\mu z}$	$R_{\mu z}$	$E_{\mu z}$	P_{DOC}
Extr. microb.	2.11	1.97	0.63	0.16	0.56	**0.36**	**0.18**	**0.26**	0.36
Microbial	2.09	1.93	0.61	0.15	0.55	**0.33**	**0.16**	**0.24**	0.33
Multivorous	2.02	1.83	0.56	0.15	0.54	0.25	0.12	0.19	0.25
Herbivorous	1.91	1.68	0.47	0.14	0.51	0.14	0.07	0.10	**0.14**
Extr. herb.	1.85	1.59	0.41	0.14	0.49	0.06	0.03	0.05	**0.06**

Sensitivity analysis

To assess the sensitivity of the model (without viral lysis of bacteria) to the choice of values for key parameters, we increased or decreased by 20% BGE (Eq. A1), $GGE_{\mu z}$ (Eq. A4), NGE_{mz} (Eq. A11), $E_{\mu z}/(E_{\mu z} + R_{\mu z}) = 0.6$ (Eq. A6), $AE_{mz} \times E_{mz}/(E_{mz} + R_{mz}) = 0.23$ (Eq. A14), and $AE_{mz} = 0.7$. Table A8 shows the effects of these changes on the same modeled flows as in Table 6, for the 5 planktonic food webs at 15°C. Values in Table A8 that differ from those in Table 6 by ≥15% are in bold. The results discussed in the next paragraph are relative to the 3 non-extreme food webs.

Most of the flows in Table A8a to f are quite insensitive to changes in parameter values, and only a few show a difference ≥15%. The BACT and µZOO flows and heterotrophic DOC production (P_{DOC}) are quite insensitive to the 2 MZOO parameters, i.e. NGE_{mz} and $AE_{mz} \times E_{mz}/(E_{mz} + R_{mz})$. In contrast, the BACT flow P_b is sensitive to changes in BGE (Table A8a). The 3 µZOO flows ($P_{\mu z}$, $R_{\mu z}$, and $E_{\mu z}$) are sensitive to changes in $GGE_{\mu z}$ (Table A8b), and $R_{\mu z}$ and $E_{\mu z}$ are sensitive to $E_{\mu z}/(E_{\mu z} + R_{\mu z})$ (Table A8d). Heterotrophic DOC production is sensitive to changes in AE_{mz}, which, in turn, influences P_b and R_b in the herbivorous food web (Table A8f). According to Table A8, the sensitivity of our model to its parameters is as follows: $AE_{mz} > E_{\mu z}/(E_{\mu z} + R_{\mu z}) > BGE > GGE_{\mu z} > AE_{mz} \times E_{mz}/(E_{mz} + R_{mz}) > NGE_{mz}$.

To assess the sensitivity of the model with viral lysis of bacteria (Eqs. A19 to A21) to the choice of value for parameter BLMF (Eq. A18), we increased or decreased by 20% BLMF = 0.4. Table A9 shows the effects of these changes on the same modeled flows as in the bottom part of Table A4, for the 5 planktonic food webs at 15°C. Values in Table A9 (except L_b) differ from those in Table A4 by <15%, indicating that our model is not very sensitive to the value of parameter BLMF.

Table A8a. Sensitivity analysis. Modeled flows (without viral lysis of bacteria) were computed with BGE = 0.218 at 15°C (Eq. A1) being increased and decreased by 20%. Values below are compared with those in the last 5 rows of Table 6 (i.e. modeled flows, with standard parameters), and differences ≥15% are in bold

Food web	I_C	A_C	P_C	P_b	R_b	$P_{\mu z}$	$R_{\mu z}$	$E_{\mu z}$	P_{DOC}
BGE + 20%									
Extr. microb.	2.29	2.14	0.75	**0.18**	0.51	0.44	0.22	0.32	0.49
Microbial	2.26	2.09	0.72	**0.18**	0.50	0.40	0.20	0.30	0.48
Multivorous	2.17	1.97	0.65	**0.17**	0.48	0.31	0.15	0.23	0.45
Herbivorous	2.04	1.78	0.53	**0.16**	0.44	0.16	0.08	0.12	0.40
Extr. herb.	1.95	1.66	0.46	**0.15**	0.42	**0.07**	**0.03**	**0.05**	0.37
BGE – 20%									
Extr. microb.	2.15	2.01	0.64	**0.11**	0.54	0.41	0.20	0.30	0.46
Microbial	2.12	1.97	0.62	**0.11**	0.53	0.37	0.18	0.27	0.44
Multivorous	2.04	1.85	0.55	**0.11**	0.51	0.28	0.14	0.21	0.42
Herbivorous	1.92	1.67	0.44	**0.10**	0.47	0.13	0.07	0.10	0.37
Extr. herb.	1.84	1.55	0.38	**0.10**	0.45	**0.04**	**0.02**	**0.03**	0.35

Table A8b. Sensitivity analysis. Modeled flows (without viral lysis of bacteria) were computed with $GGE_{\mu z} = 0.45$ at 15°C (Eq. A4) being increased and decreased by 20%. Values below are compared with those in the last 5 rows of Table 6 (i.e. modeled flows, with standard parameters), and differences ≥15% are in bold

Food web	I_C	A_C	P_C	P_b	R_b	$P_{\mu z}$	$R_{\mu z}$	$E_{\mu z}$	P_{DOC}
$GGE_{\mu z}$ + 20%									
Extr. microb.	2.31	2.14	**0.79**	0.14	0.51	**0.51**	**0.17**	**0.26**	0.45
Microbial	2.27	2.09	0.76	0.14	0.50	**0.46**	**0.16**	**0.24**	0.44
Multivorous	2.17	1.95	0.67	0.13	0.48	**0.35**	**0.12**	**0.18**	0.42
Herbivorous	2.01	1.74	0.52	0.13	0.45	**0.18**	**0.06**	**0.09**	0.38
Extr. herb.	1.91	1.61	0.43	0.12	0.44	**0.07**	**0.02**	**0.03**	0.36
$GGE_{\mu z}$ – 20%									
Extr. microb.	2.13	2.01	**0.59**	0.15	0.54	**0.34**	**0.24**	**0.37**	0.49
Microbial	2.11	1.97	0.57	0.15	0.53	**0.31**	**0.22**	**0.33**	0.48
Multivorous	2.04	1.87	0.53	0.14	0.51	**0.24**	**0.17**	**0.25**	0.45
Herbivorous	1.94	1.70	0.45	0.13	0.47	**0.12**	**0.08**	**0.13**	0.39
Extr. herb.	1.88	1.59	0.40	0.12	0.44	**0.04**	**0.03**	**0.05**	0.36

Table A8c. Sensitivity analysis. Modeled flows (without viral lysis of bacteria) were computed with NGE_{mz} = 0.355 at 15°C (Eq. A11) being increased and decreased by 20%. Values below are compared with those in the last 5 rows of Table 6 (i.e. modeled flows, with standard parameters). None of the differences are ≥15%

Food web	I_C	A_C	P_C	P_b	R_b	$P_{\mu z}$	$R_{\mu z}$	$E_{\mu z}$	P_{DOC}
NGE_{mz} + 20%									
Extr. microb.	2.23	2.09	0.71	0.14	0.52	0.42	0.21	0.31	0.46
Microbial	2.20	2.04	0.69	0.14	0.51	0.39	0.19	0.28	0.45
Multivorous	2.12	1.93	0.62	0.14	0.48	0.29	0.14	0.22	0.42
Herbivorous	2.00	1.74	0.52	0.12	0.45	0.15	0.07	0.11	0.37
Extr. herb.	1.92	1.63	0.46	0.12	0.42	0.05	0.03	0.04	0.34
NGE_{mz} – 20%									
Extr. microb.	2.21	2.06	0.67	0.15	0.53	0.43	0.21	0.31	0.48
Microbial	2.18	2.02	0.64	0.15	0.52	0.39	0.19	0.29	0.47
Multivorous	2.09	1.89	0.57	0.14	0.50	0.30	0.15	0.22	0.44
Herbivorous	1.95	1.70	0.45	0.13	0.47	0.15	0.07	0.11	0.40
Extr. herb.	1.87	1.58	0.38	0.13	0.45	0.06	0.03	0.04	0.38

Table A8d. Sensitivity analysis. Modeled flows (without viral lysis of bacteria) were computed with $E_{\mu z}/(E_{\mu z} + R_{\mu z})$ = 0.6 (Eq. A6) being increased and decreased by 20%. Values below are compared with those in the last 5 rows of Table 6 (i.e. modeled flows, with standard parameters), and differences ≥15% are in bold

Food web	I_C	A_C	P_C	P_b	R_b	$P_{\mu z}$	$R_{\mu z}$	$E_{\mu z}$	P_{DOC}
$E_{\mu z}/(E_{\mu z} + R_{\mu z})$ + 20%									
Extr. microb.	2.32	2.17	0.72	0.16	0.58	0.43	**0.15**	**0.38**	**0.54**
Microbial	2.28	2.12	0.69	0.16	0.57	0.40	**0.14**	**0.35**	0.52
Multivorous	2.17	1.98	0.61	0.15	0.53	0.30	**0.10**	**0.26**	0.48
Herbivorous	2.01	1.75	0.50	0.13	0.48	0.15	**0.05**	**0.13**	0.41
Extr. herb.	1.91	1.61	0.42	0.12	0.44	0.06	**0.02**	**0.05**	0.37
$E_{\mu z}/(E_{\mu z} + R_{\mu z})$ – 20%									
Extr. microb.	2.13	1.99	0.67	0.13	0.47	0.42	**0.27**	**0.25**	**0.40**
Microbial	2.10	1.95	0.64	0.13	0.47	0.38	**0.24**	**0.22**	0.40
Multivorous	2.04	1.85	0.58	0.13	0.46	0.29	**0.19**	**0.17**	0.38
Herbivorous	1.94	1.69	0.48	0.12	0.44	0.15	**0.09**	**0.09**	0.36
Extr. herb.	1.88	1.59	0.42	0.12	0.43	0.05	**0.03**	**0.03**	0.35

Table A8e. Sensitivity analysis. Modeled flows (without viral lysis of bacteria) were computed with $AE_{mz} \times E_{mz}/(E_{mz} + R_{mz})$ = 0.7 × 0.33 = 0.23 (Eqs. A14 & A15) being increased and decreased by 20%. Values below are compared with those in the last 5 rows of Table 6 (i.e. modeled flows, with standard parameters). None of the differences are ≥15%

Food web	I_C	A_C	P_C	P_b	R_b	$P_{\mu z}$	$R_{\mu z}$	$E_{\mu z}$	P_{DOC}
$AE_{mz} \times E_{mz}/(E_{mz} + R_{mz})$ + 20%									
Extr. microb.	2.24	2.10	0.70	0.15	0.54	0.43	0.21	0.31	0.49
Microbial	2.21	2.05	0.67	0.15	0.53	0.39	0.19	0.29	0.48
Multivorous	2.14	1.94	0.60	0.14	0.51	0.30	0.15	0.22	0.45
Herbivorous	2.01	1.76	0.50	0.13	0.48	0.15	0.07	0.11	0.42
Extr. herb.	1.94	1.65	0.43	0.13	0.46	0.06	0.03	0.04	0.39
$AE_{mz} \times E_{mz}/(E_{mz} + R_{mz})$ – 20%									
Extr. microb.	2.20	2.06	0.69	0.14	0.51	0.42	0.21	0.31	0.46
Microbial	2.16	2.01	0.66	0.14	0.50	0.39	0.19	0.28	0.44
Multivorous	2.08	1.88	0.59	0.13	0.48	0.29	0.14	0.22	0.41
Herbivorous	1.94	1.68	0.48	0.12	0.44	0.14	0.07	0.11	0.36
Extr. herb.	1.85	1.56	0.41	0.11	0.41	0.05	0.03	0.04	0.33

Table A8f. Sensitivity analysis. Modeled flows (without viral lysis of bacteria) were computed with AE_{mz} = 0.7 (Eq. A12) being increased and decreased by 20%. Values below are compared with those in the last 5 rows of Table 6 (i.e. modeled flows, with standard parameters), and differences ≥15% are in bold

Food web	I_C	A_C	P_C	P_b	R_b	$P_{\mu z}$	$R_{\mu z}$	$E_{\mu z}$	P_{DOC}
AE_{mz} + 20%									
Extr. microb.	2.14	2.06	0.69	0.13	0.48	0.42	0.21	0.31	0.42
Microbial	2.10	2.02	0.66	0.13	0.47	0.38	0.19	0.28	0.40
Multivorous	1.99	1.89	0.59	0.12	0.44	0.29	0.14	0.21	**0.36**
Herbivorous	1.83	1.70	0.48	**0.11**	**0.39**	0.14	0.07	0.10	**0.29**
Extr. herb.	1.72	1.58	0.41	**0.10**	**0.35**	**0.04**	**0.02**	**0.03**	**0.25**
AE_{mz} – 20%									
Extr. microb.	2.32	2.09	0.70	0.16	0.57	0.43	0.21	0.32	0.53
Microbial	2.30	2.04	0.67	0.16	0.57	0.40	0.19	0.29	**0.53**
Multivorous	2.24	1.93	0.60	0.16	0.56	0.30	0.15	0.22	**0.52**
Herbivorous	2.15	1.75	0.49	**0.15**	**0.54**	0.16	0.08	0.12	**0.50**
Extr. herb.	2.09	1.63	0.43	**0.15**	**0.53**	**0.07**	**0.03**	**0.05**	**0.48**

Table A9. Sensitivity analysis. Modeled flows (with viral lysis of bacteria) were computed for with BLMF = 0.4 (Eq. A18) being increased and decreased by 20%. Values below are compared with those in the last 5 rows of Table A4 (i.e. modeled flows, with BLMF = 0.4), and differences ≥15% are in bold

Food web	I_C	A_C	P_C	P_b	R_b	L_b	$P_{\mu z}$	$R_{\mu z}$	$E_{\mu z}$	P_{DOC}
BLMF + 20%										
Extr. microb.	2.16	2.02	0.59	0.08	0.56	**0.07**	0.40	0.19	0.29	0.44
Microbial	2.12	1.97	0.56	0.08	0.55	**0.07**	0.36	0.18	0.26	0.43
Multivorous	2.05	1.86	0.50	0.08	0.53	**0.07**	0.27	0.13	0.20	0.40
Herbivorous	1.92	1.67	0.40	0.07	0.49	**0.07**	0.12	0.06	0.09	0.36
Extr. herb.	1.84	1.56	0.33	0.07	0.46	**0.06**	0.03	0.01	0.02	0.33
BLMF – 20%										
Extr. microb.	2.18	2.04	0.62	0.10	0.55	**0.05**	0.41	0.20	0.30	0.45
Microbial	2.15	1.99	0.60	0.10	0.54	**0.05**	0.37	0.18	0.27	0.44
Multivorous	2.07	1.88	0.53	0.10	0.51	**0.05**	0.28	0.14	0.20	0.41
Herbivorous	1.94	1.69	0.43	0.09	0.48	**0.04**	0.13	0.06	0.10	0.37
Extr. herb.	1.86	1.57	0.36	0.09	0.46	**0.04**	0.04	0.02	0.03	0.34

Microbial-hub approach: summary flows

The following equations show the calculation of the 5 summary flows in the microbial-hub approach [i.e. R_{met}, R_{hub}, $R_{met}(PP_T)$, $R_{hub}(PP_T)$, and R_{met}(hub); Fig. 5c], using values of PP and of modeled flows from the original food-wed model (Table 6). In the equations below (as in the text and elsewhere in Appendices 1 & 2), PP_D, PP_P, and all modeled or calculated flows are expressed as fractions of PP_T or R_C ($PP_T = R_C$), and $PP_{P\mu z}$ and PP_{Pmz} are expressed as fractions of PP_P.

The equations to compute the 5 summary flows are as follows. Fig. 5c shows that:

$$R_{met}(PP_T) + R_{hub}(PP_T) = 1 \quad \text{(A24)}$$

$$R_{met}(PP_T) + R_{met}(\text{hub}) + R_{hub} = 1 \quad \text{(A25)}$$

$$R_{met} + R_{hub} = 1 \quad \text{(A26)}$$

Using Eqs. (A24) to (A26) and Fig. 5a,b, it can be shown that METAZ respiration is:

$$R_{met}\ (\text{Fig. 4c}) = R_{mz} + R_{large}\ (\text{Fig. 5a, b}) \quad \text{(A27)}$$

HUB respiration is:

$$R_{hub}\ (\text{Fig. 5c}) = R_{\mu z} + R_b\ (\text{Fig. 5a, b}) = 1 - R_{met}\ (\text{Eq. A26}) \quad \text{(A28)}$$

The direct METAZ channeling of PP_T toward R_C is:

$$R_{met}(PP_T)\ (\text{Fig. 5c}) = PP_{Tmz}\ (\text{Fig. 5b}) = PP_P \times PP_{Pmz}\ (\text{Fig. 5a}) \quad \text{(A29)}$$

The total direct HUB channeling of PP_T toward R_C is:

$$R_{hub}(PP_T)\ (\text{Fig. 5c}) = PP_{T\mu z} + PP_D\ (\text{Fig. 5b}) = (PP_P \times PP_{P\mu z}) + PP_D\ (\text{Fig. 5a}) = 1 - R_{met}(PP_T)\ (\text{Eq. A24}) \quad \text{(A30)}$$

The difference between the channeling of carbon by HUB toward METAZ R, and by METAZ toward HUB R is:

$$R_{met}(hub)\ (Fig.\ 5c), = P_{\mu z} - (D_b + E_{mz})\ (Fig.\ 5a,b)$$
$$= 1 - [R_{met}(PP_T) + R_{hub}]\ (Eq.\ A25)$$
$$= R_{met} - R_{met}(PP_T) = R_{hub}(PP_T) - R_{hub} \quad (A31)$$

Positive $R_{met}(hub)$ values represent a net transfer of carbon from HUB toward METAZ R, and negative values represent a net transfer of carbon from METAZ toward HUB R. Eqs. (A27) to (A31) were used to compute the summary flows in Tables 8 & 9.

Appendix 2. Food-web and biogeochemical considerations

Effects of viral lysis on bacterial growth efficiency

The usual field methods for estimating P_b (i.e. incorporation of radio-labeled leucine or thymidine in bacterial proteins or nucleic acids, respectively, and the appropriate biomass conversion factors) quantify the increase in bacterial biomass during the incubation period. Since the production of biomass can occur only with accompanying uptake of organic carbon, the computed or observed increase in biomass for a bacterial population is the net value of both the loss of cellular material (i.e. L_b) and the use of organic carbon in catabolic processes (i.e. R_b):

$$P_b = A_b - (R_b + L_b) \quad (A32)$$

Hence, net changes in biomass (Eq. A32; equations with 'A' designations are in the Appendices; those without are in the text) take into account the effect of L_b on the bacterial compartment as described in Eq. (4).

The effect of L_b on bacterial growth efficiency (BGE) depends on how BGE was computed. As explained in the text (Eqs. 9 & 10), there are generally 2 ways to estimate BGE. In the first one, the denominator of BGE is $(P_b + R_b)$; thus, Eq. (9) is formulated:

$$BGE_1 = P_b / (P_b + R_b)$$

The second way to estimate BGE, is when the denominator represents substrate assimilation or uptake, which is functionally equivalent to $(P_b + R_b + L_b)$, or as given in Eq. (10):

$$BGE_2 = (P_b + L_b) / A_b = (P_b + L_b) / (P_b + R_b + L_b)$$

The following equation shows that for the same P_b and R_b, $BGE_1 > BGE_2$:

$$BGE_1{:}BGE_2 = (P_b \times A_b) / [(P_b \times A_b) + (R_b \times L_b)] < 1.0 \quad (A33)$$

Since the magnitude of L_b and mortality due to microzooplankton grazing (which in our model is equal to P_b) may be similar (see the section 'Components of a generalized planktonic food-web model–Effects of DOC released from bacteria'), the effect of L_b on estimates of BGE could be large.

As explained in the text, R_b is generally computed with Eq. (11) (e.g. del Giorgio & Cole 2000, Rivkin & Legendre 2001) as follows:

$$R_b = (P_b / BGE_1) - P_b$$

Eq. (11) is correct when $BGE = BGE_1$ (Eq. 9). Hence, R_b requires estimates of P_b and BGE_1. It does not require an estimate of L_b.

In cases where the reported $BGE = BGE_2$ (Eq. 10), R_b is computed as follows:

$$R_b = [(P_b + L_b) / BGE_2] - (P_b + L_b) \quad (A34)$$

When using Eq. (A34), BGE_2, P_b, and L_b must be known. R_b would be overestimated if computed using BGE_2 and Eq. (11), i.e. neglecting the effect of L_b.

Use of P_x:*PP* instead of R_x:*PP*

The occurrence of P_x:*PP* values in the literature suggests that, even if other ecosystem properties than R are not additive, P_x:*PP* contains useful and diagnostic food-web information, e.g. for comparing either a given food-web compartment under different environmental conditions or different food-web compartments within a given system. This section shows that this is not the case, and that using P_x:*PP* instead of R_x:*PP* biases the characterization of food-web relationships.

What is the influence of using P_x:*PP* instead of R_x:*PP* to compare a given food-web compartment under different environmental conditions? We consider this situation for BACT with the same R_b:*PP* at 3 temperatures (i.e. T = 5, 15, and 25°C; the ratio of R_b:*PP* among the 3 temperatures would be 1:1:1). Using Eq. (11) and Eq. (A1) gives (P_b:*PP*):(R_b:*PP*) = 0.48, 0.28, and 0.13, at 5, 15, and 25°C, respectively; the corresponding ratio

of P_b:*PP* among the 3 temperatures is 3.7:2.2:1. The latter ratio is very different from R_b:*PP* = 1:1:1. Hence, using P_x:*PP* instead of R_x:*PP* to compare the activity of a food-web compartment in various environments provides a distorted picture of the activity of that food-web compartment.

If we compare P_x:*PP* instead of R_x:*PP* for different food-web compartments within a given system, there is a similar bias to that described in the above paragraph. Let us consider the hypothetical case of a system (at 15°C) where (R_b:*PP*):($R_{\mu z}$:*PP*):(R_{mz}:*PP*) = 5:3:1. The calculations are more complex than in the previous paragraph because the dependence of GGE and NGE on environmental factors is not the same for the different compartments (i.e. Eqs. (A1), (A4) & (A11) for BGE, $GGE_{\mu z}$, and NGE_{mz}, respectively, in Electronic Appendix 1, where the growth efficiencies are expressed as a function of *T*). Using the previously cited expressions for growth efficiencies, and the appropriate equations from Appendix 1 gives, for our hypothetical case (P_b:*PP*):(R_b:*PP*) = 0.3 (Eq. 9), ($P_{\mu z}$:*PP*):($R_{\mu z}$:*PP*) = 2.0 (Eqs. A5 & A9), and (P_{mz}:*PP*):(R_{mz}:*PP*) = 0.8 (Eqs. A10, A12, A16 & A17); the corresponding ratio of P_x:*PP*, relative to P_{mz}:*PP*, is (P_b:*PP*):($P_{\mu z}$:*PP*):(P_{mz}:*PP*):(P_{large}:*PP*) = 1.7:7.5:1. The latter ratio is very different from (R_b:*PP*):($R_{\mu z}$:*PP*):(R_{mz}:*PP*) = 5:3:1. Hence, using P_x:*PP* instead of R_x:*PP* to compare the activity of different food-web compartments within a system provides a distorted picture of the activity of these compartments.

Conditions for $A_x > PP$ in the ocean

We defined in the section 'Assessing the roles of planktonic food-web compartments–Uses and misuses of I_x:*PP*, A_x:*PP*, and R_x:*PP*' of a steady-state food web as one where the biomasses of the food-web compartments were constant. In the ocean, a second steady-state condition is that there is no net import (*M*) or export (*X*) of organic carbon from and to the euphotic zone.

In the ocean, *PP* is generally not entirely respired in the euphotic zone, i.e. some particulate organic carbon is vertically exported to depth. In addition, there is horizontal *M* and *X*. Eq. (15) summarizes the overall balance between *X*, and *M*, *PP*, and R_C:

$$X = M + PP - R_C \quad \text{(A35)}$$

In order to include *X* and *M* in our steady-state food-web model, we combined Eqs. (2 & A35):

$$A_C = P_C + E_C + PP + (M - X) \quad \text{(A36)}$$

Alternatively:

$$A_C = P_C + E_C + PP - (X - M) \quad \text{(A37)}$$

The first steady-state condition (i.e. constant biomasses) is generally achieved only at large spatial scales (e.g. ocean basins) and long temporal scales (i.e. 1 or several years). Over smaller and shorter scales, the biomasses of food-web compartments can vary, and A_C may be smaller than *PP*. The scale over which the second steady-state condition (i.e. $M = X$) is achieved is not well constrained, and it is not known if steady state may occur at the scale of ocean basins or the world ocean. For example, carbon inputs from continents via rivers (~0.25 to 0.4 Gt yr^{-1}; Probst 1992, Cauwet 2002) and the atmosphere (i.e. 1.5 to 3 Gt yr^{-1}; Duce et al. 1991, Cornell et al. 1995, del Giorgio & Duarte 2002) are in approximate balance with the vertical export of particles at ~2000 m (i.e. 1 to 2 Gt yr^{-1}; Lampitt & Antia 1997, Bauer & Druffel 1998, Antia et al. 2001).

Following, we examine contrasting non-steady-state situations where $M > X$ and $X > M$. The first case is that of waters where $M > X$, and where there is consequently net import of organic carbon [i.e. $M - X > 0$; it follows from Eq. (35) that $R_C > PP$]. Examples are near-shore waters (i.e. import of continental DOC), and areas of the ocean where $R_C > PP$ (i.e. net heterotrophic regions; to date, these areas have been identified from discrete, short-term observations). When the sum of R_C and *X* exceeds contemporaneous *PP*, an import of organic carbon is required to supplement the local *PP*; carbon may be transported by advection from regions where $R_C < [PP + (M - X)]$. In waters where $(M - X) > 0$, all terms on the right-hand side of Eq. (A36) are positive, showing that $A_C > PP$. The second case is that of regions where $X > M$ and where there is consequently net export of organic carbon (i.e. $X - M > 0$; it follows from Eq. A35 that $PP > R_C$). Examples are areas of high *PP*, where $PP > R_C$ and from which POC and/or DOC are exported downwards and/or advected laterally. For this situation, Eq. (A37) shows that $A_C > PP$ when $(X - M) < (P_C + E_C)$ and $A_C < PP$ when $(X - M) > (P_C + E_C)$. These conclusions are summarized in Table 2, which shows that the only case where $A_C < PP$ is when both $X > M$ and $(X - M) > (P_C + E_C)$. In other words, even under non-steady-state conditions, generally $A_C > PP$.

Effects of dissolved *PP* on estimates of R_x:*PP*

Values of R_x:*PP* (or R_C:*PP*) reported in the literature are often not comparable because of the use of different variables (i.e. forms of primary production) are used in the denominator. It is explained in the section 'Assessing the roles of planktonic food-web compartments–Effects of dissolved *PP* on estimates of R_x:*PP*' that, for example, R_x is generally divided by PP_P. The latter is typically determined from isotope fluxes (e.g.

$^{14 \text{ or } 13}C$ uptake or ^{18}O production), but, in some cases, it may be derived from phytoplankton growth (estimated during dilution assay experiments) that is multiplied by phytoplankton standing stock (e.g. Landry et al. 2000, Laws et al. 2000). However, the dissolved component of *PP* (i.e. PP_D) can account for a significant fraction of total *PP* ($PP_T = PP_D + PP_P$), with global medians of PP_D:PP_T (often called 'phytoplankton exudation rate' or 'percentage of extracellular release', PER) ranging between 15 and 20% (reviews by Baines & Pace 1991, Nagata 2000, Marañón et al. 2004 and references cited therein). Given that osmotrophy by bacteria is a dominant pathway of organic carbon remineralization in the sea, the denominator in any computation of the fraction of *PP* respired must include PP_D as well as PP_P (i.e. R_x:PP_T) if this ratio is to be used as a valid metric for assessing trophic conditions or comparing food-web compartments. An alternative approach (e.g. Rivkin & Legendre 2001, Robinson et al. 2002, Robinson & Williams 2005) is to divide R_x by R_C (i.e. R_x:R_C). The 3 dominators described above are not comparable: generally $PP_D > 0$, hence $PP_P \leq PP_T$, and because part of PP_T may not be respired locally (i.e. it may be exported), then $R_C \leq PP_T$. It follows that:

$$R_x{:}R_C \times R_x{:}PP_T \quad \text{(A38)}$$

and

$$R_x{:}PP_p > R_x{:}PP_T \quad \text{(A39)}$$

For example, Calbet & Landry (2004) divided $R_{\mu z}$ by PP_P, whereas Rivkin & Legendre (2001) divided R_b by R_C, and Anderson & Ducklow (2001) divided R_b by PP_T (in their steady-state model, PP_T is the same as R_C). To compare ecosystem or food-web responses using the ratio of respiration to an ecosystem property requires that the denominators be the same. Unfortunately this is frequently not done, and leads to confusion in the literature. In the case of marine ecosystems, the numerator of ratios should be R_x and the denominator should be R_C or PP_T.

Another approach to estimate R_x:*PP*, already mentioned in the section 'Assessing the roles of planktonic food-web compartments–Effects of dissolved *PP* on estimates of R_x:*PP*', was described by Calbet & Landry (2004) for microzooplankton. They computed $R_{\mu z}$:PP_P by multiplying $I_{\mu z}$:PP_P (determined from dilution experiments) by a literature-derived value of $R_{\mu z}$:$I_{\mu z}$. The resulting value of $R_{\mu z}$:PP_P depends on the specific $R_{\mu z}$:$I_{\mu z}$ used. For example, Calbet & Landry (2004) chose a constant $R_{\mu z}$:$I_{\mu z} = 0.5$, and added 5% of PP_P to account for the feeding of bacterivorous protozoans on P_b. They reported that $R_{\mu z}$:PP_P ranged from 35 to 43% over representative habitats of the world ocean. Other studies have used instead $R_{\mu z}$:$I_{\mu z} = 0.2$ (Vézina & Pace 1994, Vézina et al. 2000, Richardson et al. 2004) or $R_{\mu z}$:$I_{\mu z} = 0.42$ (Niquil et al. 1999) to model planktonic food webs in lakes, coastal waters, and the open ocean. Applying $R_{\mu z}$:$I_{\mu z} = 0.2$ or 0.4 to the $A_{\mu z}$:PP_P values of Calbet & Landry (2004; last column in their Table 1) gives $R_{\mu z}$:PP_P (computed as they did) ranging from 17 to 29% or 20 to 35%, respectively. Hence, the use of a constant $R_{\mu z}$:$I_{\mu z}$ to estimate ocean-basin scale processes must be viewed with caution, especially considering the sensitivity of $R_{\mu z}$:$I_{\mu z}$ to variations in environmental conditions (including but not limited to temperature).

Some of the main points above are illustrated in Table 3, which is discussed in the text. Anderson & Ducklow (2001) report values that are comparable to our R_b:PP_T (bottom of Fig. 4 in Anderson & Ducklow 2001; BR = R_b:R_C = R_b:PP_T) for 3 ocean areas that are assumed to be in steady state: the subarctic North Pacific, the Sargasso Sea, and the Equatorial Pacific, where R_b:R_C = 0.43, 0.52, and 0.71, respectively. These values are very similar to those in our more geographically general regions of polar, temperate, and tropical zones of the world ocean, where R_b:PP_T = 0.56, 0.52, and 0.75, respectively (Table 3).

LITERATURE CITED

Anderson TR, Ducklow HW (2001) Microbial loop carbon cycling in ocean environments studied using a simple steady-state model. Aquat Microb Ecol 26:37–49

Antia AN, Koeve W, Fischer G, Blanz T and others (2001) Basin-wide particulate carbon flux in the Atlantic Ocean: regional export patterns and potential for atmospheric CO_2 sequestration. Global Biogeochem Cycles 15:845–862

Baines SB, Pace ML (1991) The production of dissolved organic matter by phytoplankton and its importance to bacteria: patterns across marine and freshwater systems. Limnol Oceanogr 36:1078–1090

Bauer JE, Druffel ERM (1998) Ocean margins as a significant source of organic matter to the deep open ocean. Nature 392:482–485

Calbet A, Landry MR (2004) Phytoplankton growth, microzooplankton grazing, and carbon cycling in marine systems. Limnol Oceanogr 49:51–57

Cauwet G (2002) DOM in the coastal zone. In: Hansell DA, Carslson CA (eds) Biogeochemistry of marine dissolved organic matter. Academic, New York, p 579–609

Cornell S, Rendell A, Jickells T (1995) Atmospheric inputs of dissolved organic nitrogen to the oceans. Nature 376: 243–246

del Giorgio PA, Cole JJ (2000) Bacterial energetics and growth efficiency. In: Kirchman DL (ed) Microbial ecology of the oceans. Wiley-Liss, New York, p 289–325

del Giorgio PA, Duarte CM (2002) Total respiration and the organic carbon balance of the open ocean. Nature 420: 379–384

Duce RA, Liss PS, Merrill JT, Atlas EL and others (1991) The atmospheric input of trace species to the world ocean. Global Biogeochem Cycles 5:193–259

Fuhrman JA (1992) Bacterioplankton roles in cycling of organic matter: the microbial food web. In: Falkowski PG, Woodhead AD (eds) Primary productivity and biogeochemical cycles in the Sea. Plenum, New York, p 361–383

Fuhrman JA (1999) Marine viruses and their biogeochemical and ecological effects. Nature 399:541–548

Ikeda T, Motoda S (1978) Estimated zooplankton production and their ammonia excretion in the Kuroshio and adjacent seas. Fish Bull (Wash D C) 76:357–367

Ikeda T, Kanno Y, Ozaki K, Shinada A (2001) Metabolic rates of epipelagic marine copepods as a function of body mass and temperature. Mar Biol 139:587–596

Lampitt RS, Antia AN (1997) Particle flux in deep seas: regional characteristics and temporal variability. Deep-Sea Res 44:1377–1409

Landry MR, Constantinou J, Latasa M, Brown SL, Bidigare RR, Ondrusek ME (2000) Biological response to iron fertilization in the eastern equatorial Pacific (IronEx II). III. Dynamics of phytoplankton growth and microzooplankton grazing. Mar Ecol Prog Ser 201:57–72

Laws EA, Landry MR, Barber RT, Campbell C, Dickson ML, Marra J (2000) Carbon cycling in primary production bottle incubations: inferences from grazing experiments and photosynthetic studies using ^{14}C and ^{18}O in the Arabian Sea. Deep-Sea Res II 47:1339–1352

Legendre L, Rivkin RB (2005) Integrating functional biodiversity, food-web processes and biogeochemical carbon fluxes into a conceptual approach for modeling the upper ocean in a high-CO_2 world. J Geophys Res 110:C09S17.1–C09S17.17

Marañón E, Cermeño P, Fernández E, Rodríguez J, Zabala L (2004) Significance and mechanisms of photosynthetic production of dissolved organic matter in a coastal eutrophic ecosystem. Limnol Oceanogr 49:1652–1666

Nagata T (2000) Production mechanisms of dissolved organic matter. In: Kirchman DL (ed) Microbial ecology of the oceans. Wiley-Liss, New York, p 121–152

Niquil N, Arias-González JE, Delesalle B, Ulanowicz RE (1999) Characterization of the planktonic food web of Takapoto Atoll lagoon, using network analysis. Oecologia 118:232–241

Pelegrí SP, Christaki U, Dolan J, Rassoulzadegan F (1999) Particulate and dissolved organic carbon production by the heterotrophic nanoflagellate *Pteridomonas danica* Patterson and Fenchel. Microb Ecol 37:276–284

Probst JL (1992) Géochimie et hydrologie de l'érosion continentale. Mécanismes, bilan global actuel et fluctuations au cours des 500 derniers millions d'années. Sciences géologiques. Mémoires, Strasbourg 94:1–161

Richardson TL, Jackson GA, Ducklow HW, Roman MR (2004) Planktonic food webs of the equatorial Pacific at 0°, 140°W: a synthesis of EqPac time-series carbon flux data. Deep-Sea Res I 51:1245–1274

Rivkin RB, Legendre L (2001) Biogenic carbon cycling in the upper ocean: effects of microbial respiration. Science 291: 2398–2400

Robinson C, Williams P (2005) Respiration and its measurement in surface marine waters. In: del Giorgio PA, Paul A, Williams PJ Le B (eds) Respiration in aquatic ecosystems. Oxford University Press, p 147–180

Robinson C, Serret P, Tilstone G, Teira E, Zubkov MV, Rees AP, Woodward EMS (2002) Plankton respiration in the eastern Atlantic Ocean. Deep-Sea Res I 49:787–813

Strom SL, Benner R, Ziegler S (1997) Planktonic grazers are a potentially important source of marine dissolved organic carbon. Limnol Oceanogr 42:1364–1374

Wilhelm SW, Suttle CA (1999) Viruses and nutrient cycles in the sea. Bioscience 49:781–788

Vézina AF, Pace ML (1994) An inverse model analysis of planktonic food webs in experimental lakes. Can J Fish Aquat Sci 51: 2034–2044

Vézina AF, Savenkoff C, Roy S, Klein B, Rivkin R, Therriault JC, Legendre L (2000) Export of biogenic carbon and structure and dynamics of the pelagic food web in the Gulf of St. Lawrence, Part 2. Inverse analysis. Deep-Sea Res II 47:609–635